A transmigratory cup in leukocyte diapedesis both through individual vascular endothelial cells and between them

Christopher V. Carman and Timothy A. Springer

The CBR Institute for Biomedical Research, Department of Pathology, Harvard Medical School, Boston, MA 02115

The basic route and mechanisms for leukocyte migration across the endothelium remain poorly defined. We provide definitive evidence for transcellular (i.e., through individual endothelial cells) diapedesis in vitro and demonstrate that virtually all, both para- and transcellular, diapedesis occurs in the context of a novel "cuplike" transmigratory structure. This endothelial structure was comprised of highly intercellular adhesion molecule-1– and vascular cell adhesion molecule-1–enriched vertical microvilli-like projections that surrounded transmigrating leukocytes and drove redistribution of their integrins into linear tracks oriented parallel to the direction of diapedesis. Disruption of projections was highly correlated with inhibition of transmigration. These findings suggest a novel mechanism, the "transmigratory cup", by which the endothelium provides directional guidance to leukocytes for extravasation.

Introduction

Extravasation of blood leukocytes is critical for immune surveillance and a crucial first step in the development of inflammation and atherosclerosis (Springer, 1994; Ross, 1999). Two well-characterized processes, selectin-mediated rolling and integrin-mediated firm adhesion, cooperate to promote accumulation of leukocytes on the luminal surface of the vascular endothelium (Luscinskas et al., 1994; Springer, 1994). Subsequently, leukocytes actively migrate, in amoeboid fashion, across the endothelial monolayer into the interstitium, a process referred to as transendothelial migration (TEM) or diapedesis (Luscinskas et al., 1994; Springer, 1994). A variety of adhesion molecules have been identified that are important for this process. These include on leukocytes the integrins leukocyte function-associated molecule-1 (LFA-1) (αLβ2), Mac-1 (αMβ2), and very late antigen-4 (VLA-4) (α4β1), and on endothelium the immunoglobulin superfamily members intercellular adhesion molecules 1 and 2 (ICAM-1 and ICAM-2), vascular cell adhesion molecule-1 (VCAM-1), platelet/endothelial cell adhesion molecule-1 (PECAM-1), and the junctional adhesion molecules, as well as the proline-rich glycoprotein CD99 (Oppenheimer-Marks et al., 1991; Luscinskas et al., 1994; Greenwood et al., 1995; Muller, 2001; Aurrand-Lions et al., 2002). However, the central issues of how the proper leukocyte directionality to cross the endothelium is established, and the nature of the route of transendothelial passage, remain unclear and controversial (Kvietys and Sandig, 2001; Muller, 2001).

Shortly after arrest, most leukocytes spread and begin to migrate laterally over the apical surface of the endothelium (Luu et al., 1999). At some point, usually within several minutes (Luu et al., 1999), leukocytes make the critical "decision" to migrate in the direction perpendicular to the plane of the endothelium and extravasate. It has been suggested that shear forces provided by the luminal circulation may help to establish this directionality (Cinamon et al., 2001), though robust diapedesis is also observed in many systems in the absence of shear. In addition, junctionally localized gradients of chemoattractants and adhesion molecules, such as PECAM-1, CD99, and the junctional adhesion molecules, have been proposed to direct leukocytes to endothelial junctions and to provide the requisite traction to drive diapedesis at these locations (Bianchi et al., 1997; Muller, 2001, 2003; Aurrand-Lions et al., 2002). Furthermore, intra-endothelial cell signaling events are thought to facilitate leukocyte passage by transiently and locally down-regulating the integrity of the endothelial adherence junctions (Huang et al., 1993; Bianchi et al., 1997; Adamson et al., 1999; Etienne-

Correspondence to Timothy A. Springer: springeroffice@cbr.med.harvard.edu

The online version of this article contains supplemental material.

Abbreviations used in this paper: BAPTA-AM, 1,2Bis(2-aminophenoxy)ethane-*N*,*N*,*N*′,*N*′-tetraacetic acid tetrakis(acetoxymethyl ester); HUVEC, human umbilical vein endothelial cell; ICAM-1, intercellular adhesion molecule-1; IRM, interference reflection microscopy; LFA-1, leukocyte function-associated molecule-1; MCP-1, monocyte chemoattractant protein-1; PAF, platelet activating factor; PECAM-1, platelet/endothelial cell adhesion molecule-1; SDF-1, stromal cell–derived factor-1; TEM, transendothelial migration; VCAM-1, vascular cell adhesion molecule-1; VLA-4, very late antigen-4.

The Journal of Cell Biology, Vol. 167, No. 2, October 25, 2004 377–388
http://www.jcb.org/cgi/doi/10.1083/jcb.200404129

Supplemental Material can be found at:
http://www.jcb.org/cgi/content/full/jcb.200404129/DC1

Manneville et al., 2000; Aurrand-Lions et al., 2002; Muller, 2003). Although all of these proposed mechanisms have merits, several considerations suggest that additional or alternate mechanism may also be important for physiologic extravasation.

First, the proposal that chemoattractants become preferentially distributed to endothelial junctions as a consequence of junctional "leakage" from the interstitium remains unsubstantiated. On the contrary, the studies to date that have carefully examined this issue in vivo, using transmission EM, demonstrate a distinct absence of junctional leakage of the chemokines IL-8 and RANTES (Middleton et al., 1997) or of EBV-induced molecule 1 ligand CC chemokine (Baekkevold et al., 2001), in postcapillary and high endothelial venules, respectively. Instead, these chemokines were shown to cross the endothelium via caveolar transcytosis, which resulted in selective presentation of chemokines on the apical microvilli (Middleton et al., 1997; Baekkevold et al., 2001). Moreover, although apically associated stromal cell–derived factor-1 (SDF-1) has been shown to be important for efficient lymphocyte diapedesis, a chemokine gradients per se was not required (Cinamon et al., 2001).

Second, models involving junctionally localized adhesion molecules are predicated on physiologic leukocyte diapedesis occurring at endothelial cell–cell junctions, i.e., the paracellular route of TEM (Bianchi et al., 1997; Muller, 2001, 2003; Aurrand-Lions et al., 2002). In the absence of conclusive observations made in the widely used in vitro cultured endothelial monolayer systems, the idea of nonjunctional TEM directly through individual endothelial cells, i.e., the transcellular route of TEM, has remained largely disregarded (Kvietys and Sandig, 2001; Muller, 2001). However, some of the very first EM studies to address the nature of TEM in vivo provided evidence for the predominance of the transcellular route of diapedesis (Williamson and Grisham, 1961; Marchesi and Gowans, 1964). Conclusive proof for transcellular migration in vivo has been provided by both serial-section transmission (Marchesi and Gowans, 1964; Cho and De Bruyn, 1986; Greenwood et al., 1994; Feng et al., 1998, 2002) and scanning (Faustmann and Dermietzel, 1985; Cho and De Bruyn, 1986; Hoshi and Ushiki, 1999) EM studies. Clearly, such events should be independent of junctional chemoattractant and/or adhesion-molecule gradients and would not require mechanisms for separation of adherence junctions.

Proactive roles for the endothelium in facilitating diapedesis have been suggested by a variety of studies. For example, disruption of the cytoskeleton or blockade of intracellular calcium in the endothelium significantly reduces the rate and extent of leukocyte diapedesis without altering firm adhesion (Huang et al., 1993; Adamson et al., 1999; Etienne-Manneville et al., 2000; Strey et al., 2002). Recently, we and others (Barreiro et al., 2002; Carman et al., 2003) have demonstrated that, as a consequence of binding to LFA-1 and VLA-4, respectively, the endothelium proactively generates ICAM-1– and VCAM-1–enriched upright microvilli-like projections that surround a portion of the adherent leukocytes. However, in neither of these studies was any relationship between projections and leukocyte TEM characterized. Rather, in one of these, the projections were described explicitly as firm adhesion "docking structures" that were predicted to be inhibitory for diapedesis and thus speculated to undergo disassembly or disruption before diapedesis could proceed (Barreiro et al., 2002). Alternatively, we directly demonstrated that inhibition of projection formation did not alter the strength of adhesion and, based on this and the kinetics of endothelial projection formation, hypothesized a role for these structures in leukocyte diapedesis (Carman et al., 2003).

Here, we make extensive use of high resolution fluorescence imaging techniques to explore the route and mechanisms for diapedesis. We demonstrate unambiguously that leukocytes can use the transcellular route of diapedesis. Furthermore, both paracellular and transcellular TEM are associated with highly ICAM-1– and VCAM-1–enriched endothelial projections which appear to play a role in guiding leukocyte extravasation.

Results

Leukocytes transmigrate through both para- and transcellular routes

To investigate the mechanism and route of leukocyte diapedesis, we established an in vitro system for imaging TEM of primary leukocytes. TNF-α–activated human umbilical vein endothelial cell (HUVEC) monolayers were treated with monocyte chemoattractant protein-1 (MCP-1) before addition of monocytes, with platelet activating factor (PAF) before addition of neutrophils, or with SDF-1 before addition of lymphocytes. Chemoattractant not associated with the monolayers was removed by washing and leukocytes were then incubated with the monolayers for various times followed by fixation and staining with antibodies to ICAM-1, LFA-1, and VE-cadherin, a specific marker for endothelial adherence junctions (Lampugnani et al., 1992). Samples were analyzed by high resolution, serial-sectioning confocal microscopy, coupled to digital deconvolution and three-dimensional image reconstruction, and leukocyte TEM was assessed according to the criteria described in Materials and methods.

At time periods of 10 min, significant numbers of all three classes of leukocytes were observed to be in the process of TEM. Remarkably, considerable fractions of TEM events were found to take place at sites clearly distinct from cell–cell junctions, demonstrating unambiguous use of the transcellular route of TEM (Fig. 1; Fig. S1, cell 2; Fig. S2, available at http://www.jcb.org/cgi/content/full/jcb.200404129/DC1). To analyze this statistically, at least 100 leukocytes in randomly selected fields from each of at least three separate experiments were imaged in all apical to basal planes. This revealed that 7 ± 1%, 5 ± 2%, and 11 ± 4% of the transmigrating monocytes, neutrophils, and lymphocytes, respectively, used transcellular routes. The remainder of leukocytes transmigrated at sites closely juxtaposed to endothelial cell–cell junctions, and were scored as paracellular TEM (Fig. 2; Fig. S1, cell 1; Fig. S2). Among the TEM events scored as paracellular, were many whose appearance was suggestive of a transcellular route, yet whose TEM passage was too close to endothelial cell–cell junctions for an unambiguous determination of transcellular TEM (Fig. S2 C).

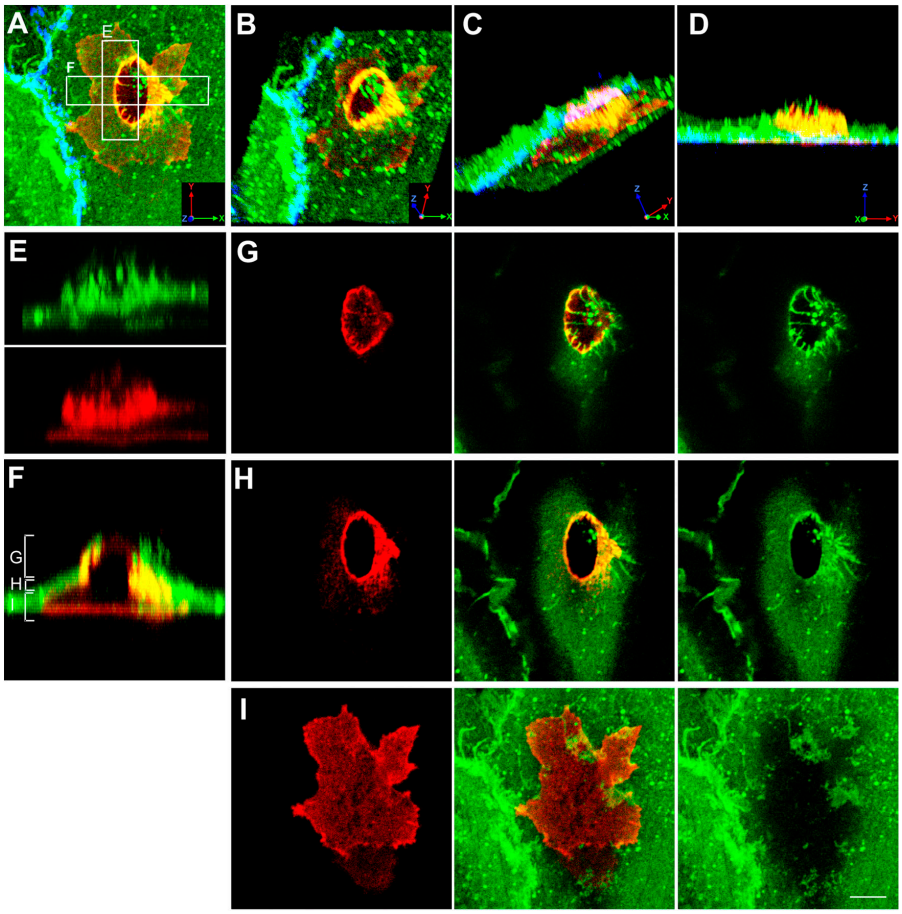

Figure 1. **Monocytes migrate across the endothelium via transcellular routes in association with ICAM-1 projections.** TNF-α–activated HUVECs were pretreated with MCP-1 and incubated with freshly isolated monocytes for 20 min. Cells were fixed and stained for ICAM-1 (CBRIC1/11-488; green), LFA-1 (CBR-LFA1/7-Cy3; red), and VE-cadherin (55-7H1-Cy5; blue; shown in A–D only) and imaged by confocal microscopy. (A) Top view projection of all z-series sections of a representative monocyte transmigrating via a transcellular route. (B–D) Field in A was rendered as a series of three-dimensional projections, each representing successive rotation about both the x and z axis in 30° intervals for a total of 90° about each axis. (E) Side view projection of cross section E in A depicting ICAM-1 projections (top) and linear LFA-1 clusters (bottom) separately. (F) Side view projection of cross section F in A. Apical (G), middle (H), or basal (I) z-axis sections, as indicated by brackets in F, are projected as top views. Bar, 5 μm.

The nature of the transcellular pore itself remains to be elucidated. However, as an initial step, we characterized the distribution of endothelial caveolin-1, a structural constituent of caveolea. These experiments demonstrate a partial, nonetheless unambiguous, association of caveolin-1 with the transcellular pore (Fig. 3), which is consistent with a potential relationship between caveolae and pore formation.

Leukocyte transmigration is highly associated with endothelial "cuplike" structures enriched in ICAM-1

The overall appearance of the endothelium and of the leukocytes was not significantly different among para- and transcellular TEM events and among monocytes, neutrophils, and lymphocytes (Figs. 1 and 2; Figs. S1 and S2). Most importantly, virtually all TEM events shared a previously unrecognized characteristic of being associated with upright microvilli-like ICAM-1–enriched endothelial projections that formed a cuplike structure that surrounded the site of diapedesis in a largely symmetrical fashion (Figs. 1 and 2; Figs. S1 and S2). This architecture was not altered when leukocytes were subjected to a wall shear stress of 4 dyne/cm^2 in a laminar flow chamber during transmigration (Fig. S3, available at http://www.jcb.org/cgi/content/full/jcb.200404129/DC1).

Close investigation of leukocyte β2 integrin, the common subunit of the ICAM-1 receptors LFA-1 and Mac-1, revealed regions of increased density that formed linear clusters oriented parallel to the direction of diapedesis, which colocalized with the ICAM-1 projections (Fig. 1 E; Fig. 2 E; and Fig. 6 C, bottom). Separate analysis of αL and αM subunits revealed similar results (unpublished data). As demonstrated previously (Carman et al., 2003), leukocytes not associated with projections failed to exhibit linear integrin clusters (unpublished data).

To quantify the relationship between the cuplike structures and diapedesis, populations of leukocytes were scored using a system similar to one described previously (Sandig et al., 1997), as either adherent but not transmigrating (i.e., completely apical), in TEM stage-1 (TEM-1; ~1–25% across the endothelium), TEM-2 (~25–75% across the endothelium), TEM-3 (75–99% across the endothelium) or under the endothelium (100% below the endothelium). In addition, each cell was scored for the presence of significant ICAM-1–enriched projections of 1 μm in length or greater, and as transmigrating via either a para- or transcellular route.

Over a 60-min time course, the fraction of monocytes that had completed diapedesis steadily increased (Fig. 4 A). At all time points the population of cells that were in any stage of TEM (TEM-1, -2, or -3) was highly associated with ICAM-1 projections (average projection-positive fraction was 96%). Consistent with our previous findings (Carman et al., 2003), a proportion of cells on the apical surface of the endothelium that had not yet initiated diapedesis were also associated with

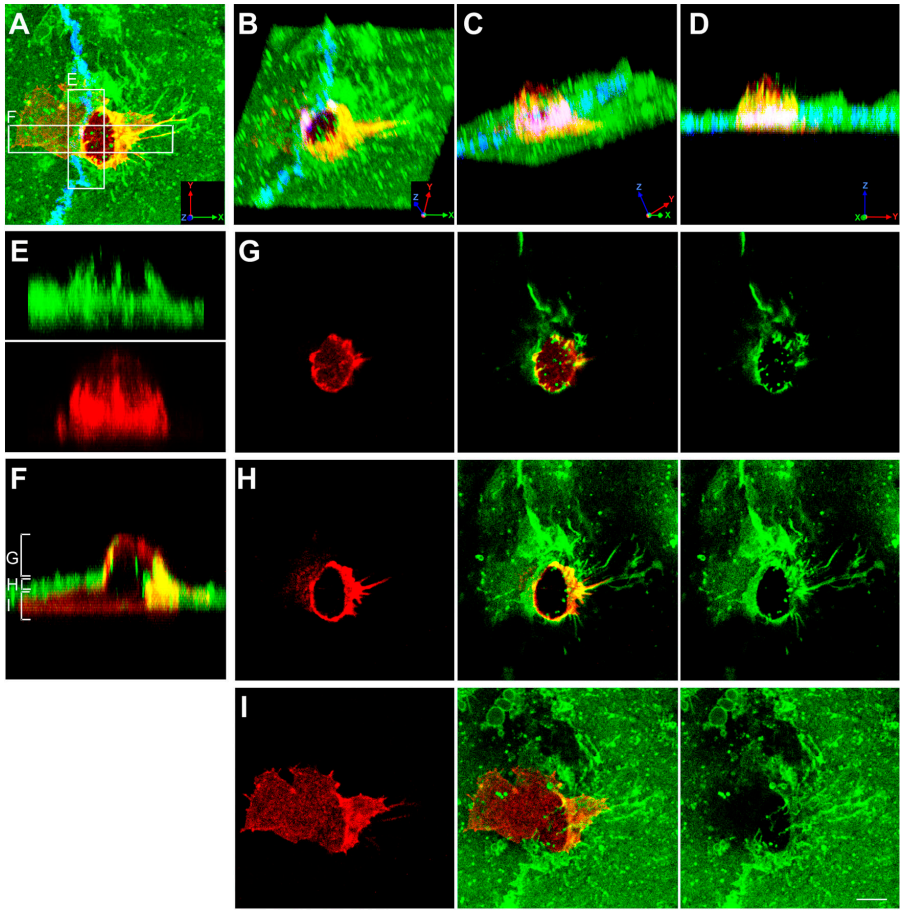

Figure 2. **Monocytes migrate across the endothelium via paracellular routes in association with ICAM-1 projections.** Samples were prepared as in Fig. 1 with ICAM-1, LFA-1, and VE-cadherin (shown in A only) represented by green, red, and blue fluorescence, respectively. (A) Top view projection of all z-series sections of a representative monocyte transmigrating via a paracellular route. (B–D) Field in A was rendered as a series of three-dimensional projections, each representing successive rotation about both the x and z axis in 30° intervals for a total of 90° about each axis. (E) Side view projection of cross section of E in A depicting ICAM-1 projections (top) and linear LFA-1 clusters (bottom) separately. (F) Side view projection of cross section F in A. Apical (G), middle (H), or basal (I) z-axis sections, as indicated by brackets in F, are projected as top views. Bar, 5 μm.

ICAM-1 projections. However, the projection-positive fraction of these cells averaged only 41% (P value vs. transmigrating cells of < 0.0001) over the 60-min time course. Using a single time point, a similar analysis was performed on neutrophils and lymphocytes (Fig. 4 B), which demonstrated a nearly complete association of TEM events with ICAM-1 projections (neutrophils, 94%; lymphocytes, 98%) and a significantly lower percentage of adherent, nontransmigrating leukocytes associated with projections (neutrophils, 22% ($P < 0.0001$); lymphocytes, 23% ($P < 0.0001$)). This situation was similar under shear conditions (4 dyne/cm^2), with the majority of transmigrating monocytes (94 ± 2%), neutrophils, (87 ± 6%) and lymphocytes (91 ± 2) associated with projections.

Of the ICAM-1 projection-positive population of transmigrating leukocytes, over all time points, 97% were associated with cuplike projections that were largely symmetrical, encircling at least 240° of the circumference of the leukocytes (See Fig. 6, A–C, bottom; Fig. S4, A–C, available at http://www.jcb.org/cgi/content/full/jcb.200404129/DC1). In contrast, of the projection-positive, apically adherent, nontransmigrating leukocytes, 30–50% were associated with asymmetrically distributed, "tetherlike" projections that contacted only one side of the leukocytes and were extended several, and sometimes up to 30 microns in length (Fig. 5). In these cases the leukocytes frequently exhibited polarized shapes suggestive of lateral migration (Worthylake and Burridge, 2001; Fig. 5). The attachment point on the leukocyte was typically one to several microns above the apical surface of the endothelium, and views parallel to the substrate (Fig. 5 B, bottom) demonstrated that the projections spanned the distance between their endothelial origin and the leukocyte suspended above the endothelium. This architecture is roughly analogous to that described for selectin-mediated transient tethers formed under shear flow, with the distinction that tethers extended up from the endothelium to the reach leukocytes rather than down from the leukocyte to reach the substrate (Chen and Springer, 1999). These findings strongly suggest that tetherlike projections were asymmetric as a result of lateral leukocyte migration away from their origin on the endothelium. To confirm this, live-cell time-lapse confocal microscopy was performed. This demonstrated that the distal ends of the projections were, indeed, attached to the trailing edge of the leukocytes and extended as a consequence of leukocyte lateral migration, whereas the endothelial origin of the projections remained stationary (Fig. 5 C). Conversely, time-lapse showed that symmetric projections formed around leukocytes that were not migrating laterally (unpublished data).

The endothelial cuplike structures are highly enriched in ICAM-1 and VCAM-1, but not ICAM-2, PECAM-1, or VE-cadherin

To investigate the localization of other relevant endothelial adhesion molecules, ICAM-1 was visualized concomitantly with β2 integrin and either VCAM-1, ICAM-2, PECAM-1, or VE-cadherin. VCAM-1 was highly coenriched with ICAM-1 in

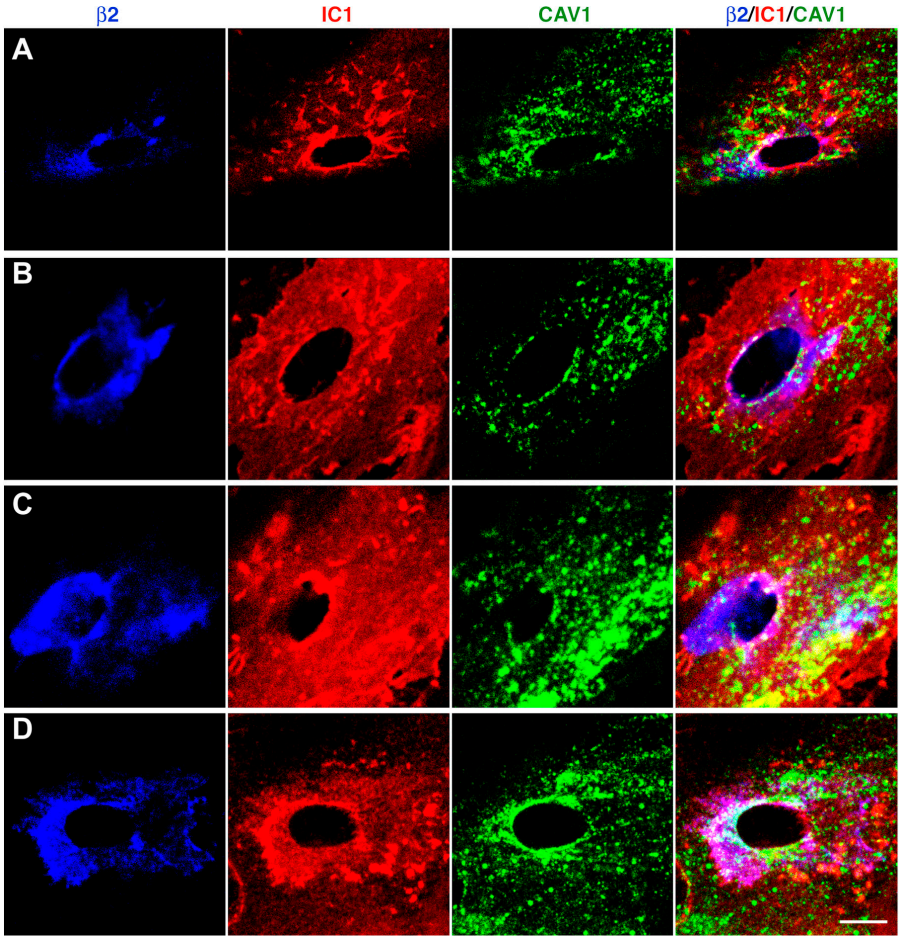

Figure 3. **Caveolin-1 is partially associated with the transcellular migration pore.** Human lymphocytes were incubated for 10 min with TNF-α–activated, SDF-1–pretreated HUVECs transfected with either caveolin-1-GFP (A and B) or GFP-caveolin-1 (C and D) followed by fixation and staining. β2 (blue), ICAM-1 (IC1; red), and caveolin-1 (cav-1; green) are shown for representative transcellular migration events. Confocal sections that encompass the TEM passage (Fig.1, F and H) are projected as top views. Bar, 5 μm.

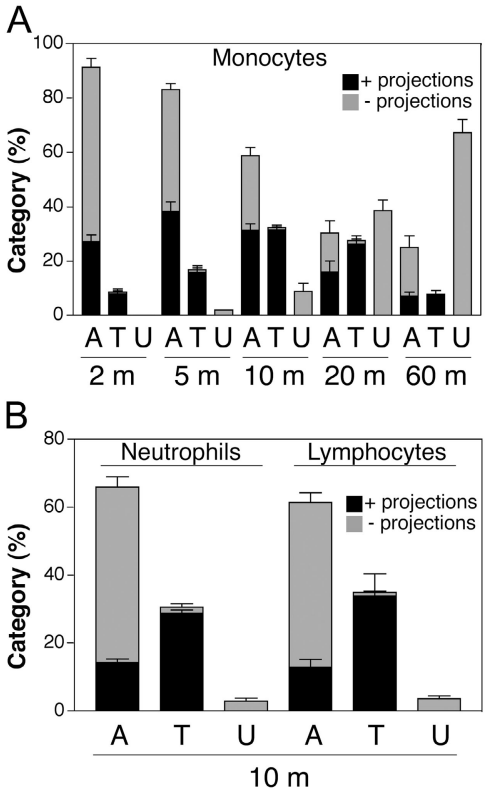

the endothelial projections surrounding both adherent (not depicted) and transmigrating leukocytes (Fig. 6, A and C; Video 1, available at http://www.jcb.org/cgi/content/full/jcb.200404129/DC1). Conversely, VE-cadherin was localized to endothelial cell–cell junctions and was absent from projections (Fig. 6 B and Fig. S4 C). Interestingly, although in the majority of the paracellular TEM events VE-cadherin staining was interrupted and absent at the site of diapedesis (Fig. 7 B; Fig. S2, A and B; Fig. S4 C), in many cases the VE-cadherin was continuous and arched around one side of the TEM passage (Fig. 2, 6B, Fig. S1,

Figure 4. **ICAM-1 projections are highly associated with transmigrating cells.** Monocytes (A) and neutrophils and lymphocytes (B) were incubated with TNF-α–activated and either MCP-1–, PAF-, or SDF-1–pretreated HUVEC monolayers, respectively, for the indicated number of minutes (m). Cells were fixed and stained for ICAM-1, LFA-1, and VE-cadherin. In each of three to eight separate experiments, a minimum of 100 leukocytes from randomly selected fields for each time point were carefully analyzed in all apical to basal planes and scored for the presence of ICAM-1–enriched projections of 1 μm in length or greater and as being either apically adherent (A), in the process of TEM (including both para- and transcellular events and including TEM stages 1–3) (T) or under (U) the HUVEC monolayer. Each bar represents the percentage of total cells scored at each indicated time point that were found in each of the three categories (i.e., A, T, or U). The black portion of each bar is the fraction of cells scored positive for associated ICAM-1 projections. The gray portion of each bar is the fraction of the cells that were negative for the presence of ICAM-1 projections. Values represent mean ± SEM (n = 3–8).

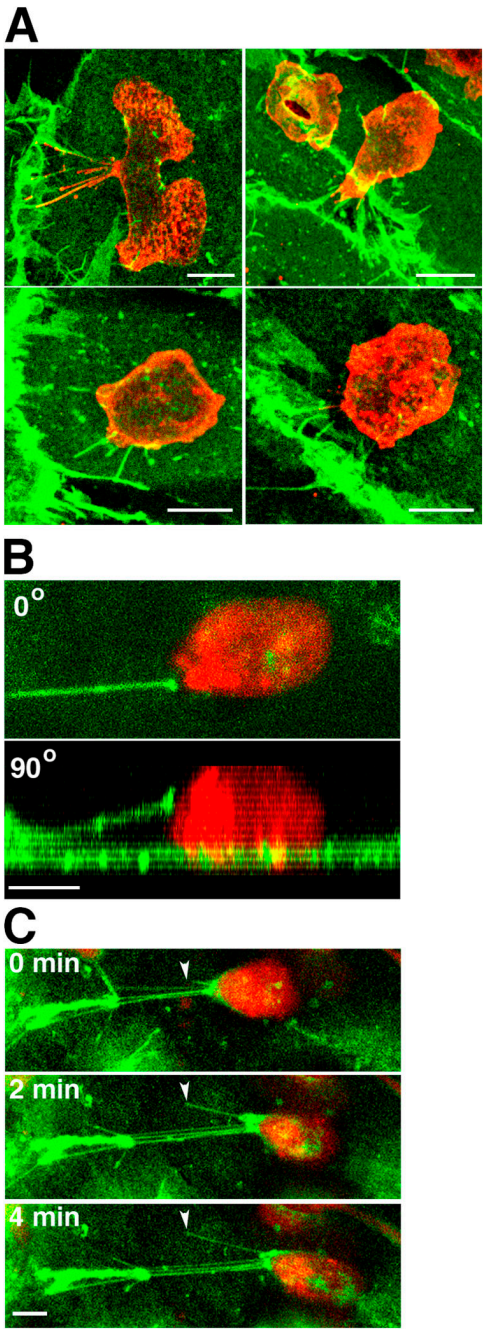

Figure 5. **Asymmetric projections are associated with laterally migrating cells.** Monocytes (A) and lymphocytes (B and C) were incubated with TNF-α–activated and either MCP-1– or SDF-1–pretreated HUVEC monolayers, respectively. (A) After 10 min of incubation cells were fixed and stained for ICAM-1 (green) and LFA-1 (red). Four representative top view images depict apically adherent monocytes with asymmetrically distributed ICAM-1 projections. (B) Live-cell imaging of a representative laterally migrating SNARF-labeled lymphocyte (red) on the apical surface of the endothelium prelabeled with an anti–ICAM-1–Alexa 488 Fab fragment (green). Image depicts top (0°; top) and side (90°; bottom) views of a single ICAM-1–bearing cellular projection that is largely suspended above the apical surface of the endothelium and is attached to a lymphocyte migrating laterally to the right. (C) Live-cell time lapse imaging of another cell as in B. ICAM-1 projections emanating from the apical surface of the endothelium (arrowheads) attached to the trailing edge of a lymphocyte become elongated as the lymphocyte advances. Panels depict top view projections of confocal sections at 0, 2, and 4 min as indicated. Bars, 5 μm.

cell 1). ICAM-2 and PECAM-1 exhibited only modest localization to the endothelial projections (Fig. S4, A and B). Functional roles for these molecules in this context cannot be excluded.

Given the strong enrichment of VCAM-1 to the projections, we also investigated the distribution of the leukocyte integrin VLA-4 (α4β1) on lymphocytes, the receptor for VCAM-1. These results revealed that α4, as with β2, αL and αM, was distributed to linear clusters on leukocytes that colocalized with the ICAM-1/VCAM-1–enriched endothelial projections (Fig. 6 D).

At initial stages of TEM, ICAM-1 projections are clearly distinct from the TEM passage

Leukocytes at initial stages of TEM (TEM-1) looked much like adherent cells (Carman et al., 2003) surrounded by a perimeter of vertical endothelial ICAM-1–enriched projections (Fig. 6 A and Fig. 7; Fig. S1, cell 2 and Fig. S3, B and C). However, at the very bottom of the leukocyte/endothelial interface, usually at the center of the perimeter of ICAM-1 projections, was a small circular/ovoid gap (~0.5-2 μm in diameter) completely devoid of ICAM-1 staining in all confocal sections (the TEM passage; Fig. 6 A and Fig. 7; Fig. S1, cell 2 and Fig. S3, B and C). LFA-1 was clearly detected within the TEM passage extending down to the most basal sections indicating a portion of the leukocyte was spread underneath the endothelium. Thus, at initial stages of TEM the vertical endothelial projections are clearly distinct from the TEM passage itself and rather form a larger perimeter that encircles the location of passage formation, as though targeting this location for diapedesis. This feature was constant for both para- and transcellular routes of TEM and for monocytes (Fig. 6 A and 7, Fig. S1, cell 2 and Fig. S3 B), neutrophils (Fig. S3 C) and lymphocytes (not depicted).

ICAM-1 projections remain associated with leukocytes through completion of diapedesis

At the late stages of TEM (TEM-3) the distal ends of the ICAM-1 projections remained well attached to the apical portion of the leukocytes with significant LFA-1 clustered underneath them (Fig. S5, A–C, available at http://www.jcb.org/cgi/content/full/jcb.200404129/DC1). At the very final stages or just after completion of TEM, the ICAM-1 projections remained attached to the LFA-1–enriched uropod of the subendothelial monocytes, neutrophils and lymphocytes. Thus, the ICAM-1 projections were often observed extending from the apical surface, through the nearly closed paracellular or transcellular TEM passage, into the basal/sub-endothelial space (Fig. S5, D–I), an assessment confirmed by parallel experiments using interference reflection microscopy (IRM; not depicted).

Conditions that attenuate formation of ICAM-1–enriched projections decrease TEM

To assess the functional role of the ICAM-1–enriched projections in TEM, we scored the relative proportions of monocytes that were adherent, transmigrating or under the HUVEC monolayer after treatment with reagents (colchicine or 1,2Bis(2-ami-

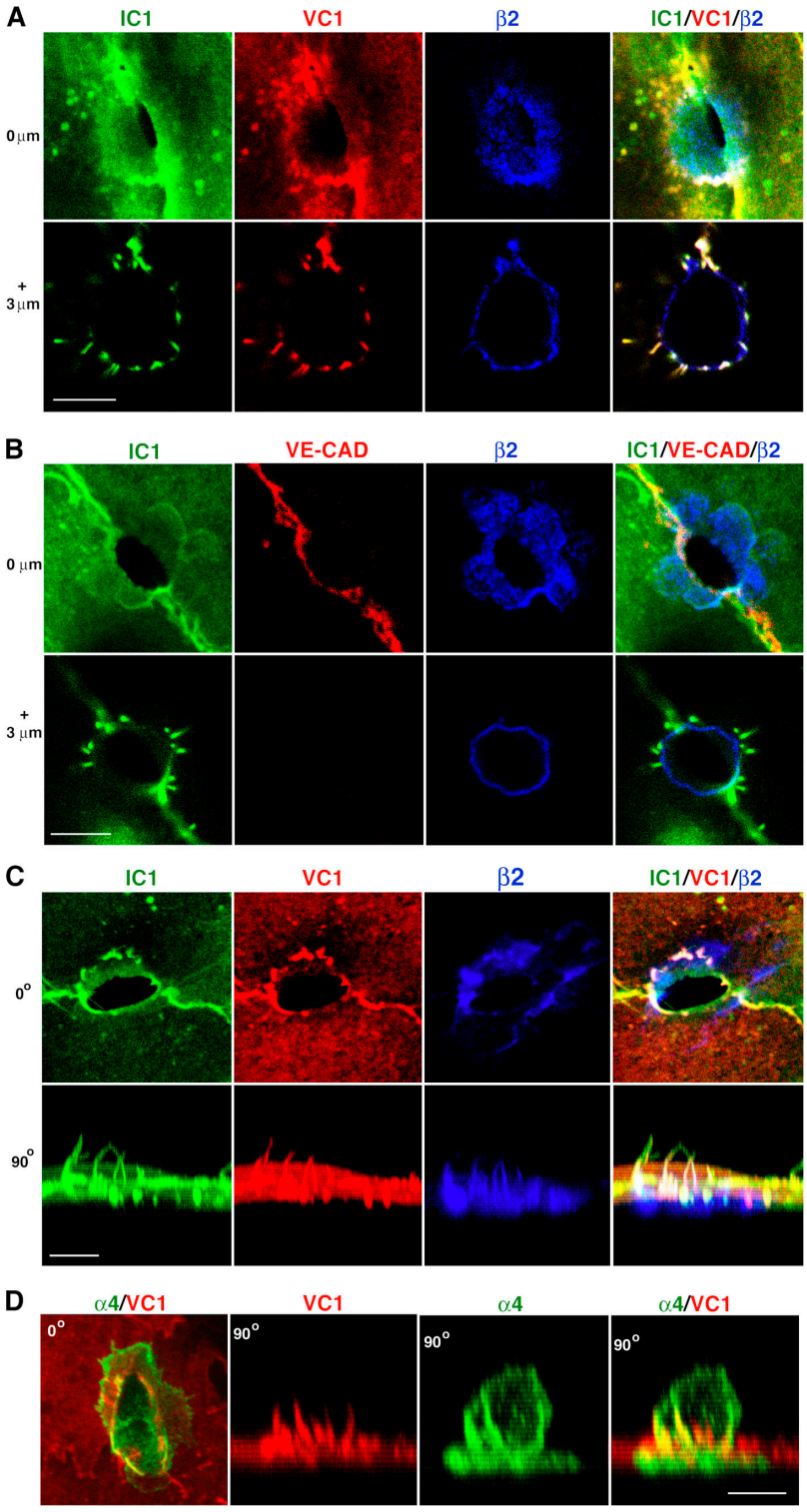

Figure 6. **ICAM-1 and VCAM-1, but not VE-cadherin, are highly enriched in projections surrounding sites of transmigration.** (A) Top view of 0.2-μm-thick confocal sections of a monocyte in TEM-1 at 0 μm (top) and 3 μm (bottom) above the apical surface of the endothelium. ICAM-1 (IC1, green), VCAM-1 (VC1, red), and β2 integrin (β2, blue) are shown either separately (left three) or merged (right). (B) Top view of confocal sections of a monocyte in TEM-1 at 0 μm (top) and 3 μm (bottom) above the apical endothelial surface. ICAM-1 (IC1, green), VE-cadherin (VE-CAD, red), and β2 integrin (β2, blue) are shown either separately (left three) or merged (right). Note that VE-cadherin staining at 0 μm is continuous at the TEM passage in contrast to Fig. S4 C. (C) Serial confocal sections of a monocyte in TEM-2 projected as top (0°, top) or side (90°, bottom) views. ICAM-1 (IC1, green), VCAM-1 (VC1, red), and β2 integrins (β2, blue) are shown either separately (left three) or merged (right). Three-dimensional rotation of these projections is shown in Video 1. (D) Serial confocal sections of a lymphocyte in TEM-2 projected as top (0°, left) or side (90°, right three) views. α4 integrin (α4, green) and VCAM-1 (VC1, red) are shown either separately (middle) or merged (left and right). Bars, 5 μm.

nophenoxy)ethane-*N*,*N*,*N*′,*N*′-tetraacetic acid tetrakis(acetoxymethyl ester); BAPTA-AM) shown previously to inhibit projections (Carman et al., 2003). Compared with controls, colchicine and BAPTA-AM significantly reduced both para- and transcellular TEM (~3-4-fold; Fig. 8 A), which is consistent with previous studies (Huang et al., 1993; Etienne-Manneville et al., 2000; J. Greenwood and P. Adamson, personal communication). Whereas 50% of adherent cells had ICAM-1 projections on the control monolayers, only 16% and 18% of the adherent cells on colchicine and BAPTA-AM treated monolayers, respectively, were associated with projections (Fig. 8 A). However, among the leukocytes that were in the process of TEM, the majority (96%, 91%, and 90% for control, colchicine, and BAPTA-AM–treated samples, respectively) were associated with ICAM-1 projections, regardless of HUVEC pretreatment (Fig. 8 A).

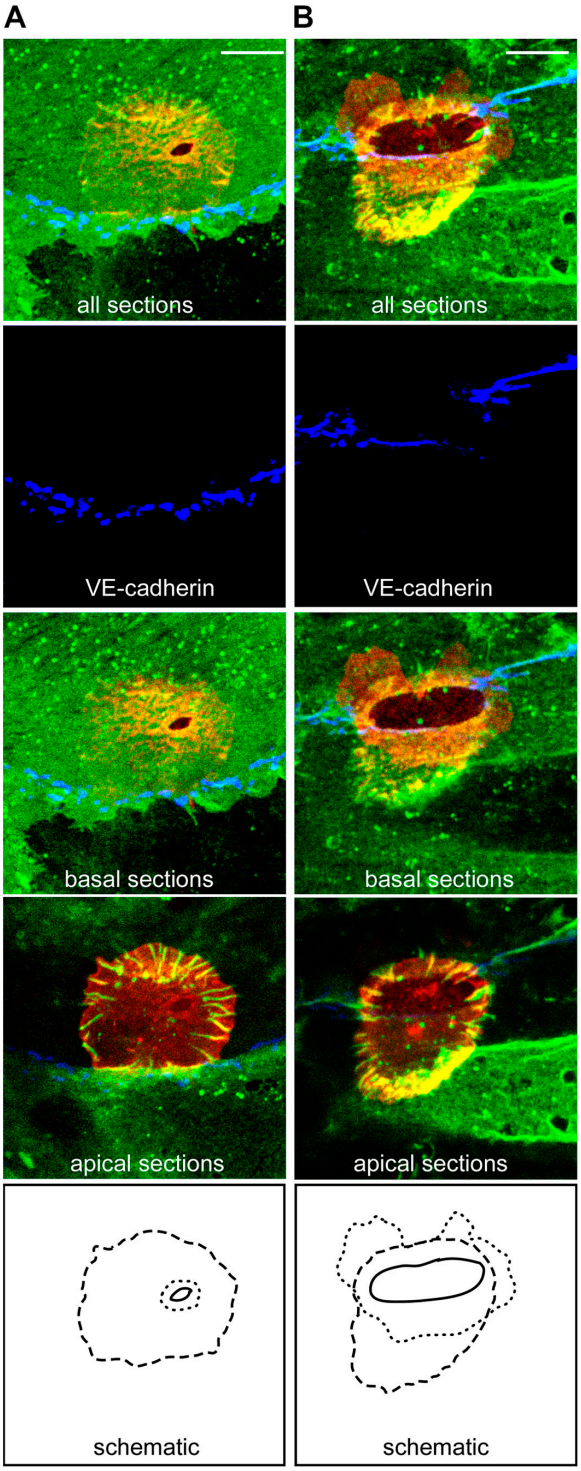

Figure 7. **At early stages of TEM ICAM-1 projections encircle the endothelial migration passage.** Monocytes were incubated with TNF-α–activated, MCP-1–pretreated HUVECs for 10–20 min and then fixed and stained for ICAM-1 (IC1/11-488, green), LFA-1 (CBR-LFA1/7-Cy3, red), and VE-cadherin (55-7H1-Cy5, blue) and imaged by confocal microscopy. (A) All sections, the basal sections or the apical sections of a representative monocyte at an early stage of transcellular TEM-1. (B) A representative monocyte at a late stage of paracellular TEM-1. Dotted, dashed, and solid lines shown in the bottom panels indicate the edges of the sub-endothelial leukocyte membrane, the perimeter of the ICAM-1 projections and the TEM passage, respectively. Note that the TEM passage resides within the perimeter established by the ICAM-1 projections. Bars, 5 μm.

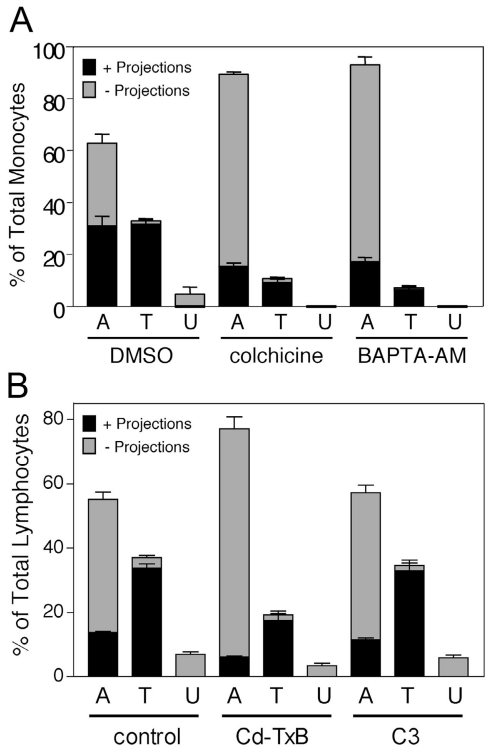

Figure 8. **Inhibition of ICAM-1 projections by BAPTA-AM, colchicine, or toxin-B is highly correlated with reduced TEM.** (A) TNF-α–activated, MCP-1–pretreated HUVECs were pretreated with vehicle (DMSO, 60 min), 10 μm colchicine (20 min), or 20 μm BAPTA-AM (60 min) washed and incubated with monocytes for 10 min at 37°C. Cells were fixed, stained for ICAM-1 (IC1/11-488), and LFA-1 (CBR-LFA1/7-Cy3) and then analyzed by confocal microscopy. In each of three to five separate experiments at least 100 monocytes in randomly selected fields were carefully analyzed in all apical to basal planes and scored for the presence of significant ICAM-1–enriched projections of 1 μm in length or greater and as being either apically adherent (A), in the process of TEM (including both para- and transcellular events and TEM 1–3) (T) or under (U) the HUVEC monolayer. Each bar represents the percentage of total cells scored for each experimental condition (DMSO, colchicine, or BAPTA-AM) in each of the three categories. The black portion of each bar is the fraction of cells positive for associated ICAM-1 projections. The gray portion of each bar is the fraction of the cells that were negative for the presence of ICAM-1 projections. (B) TNF-α–activated, SDF-1–pretreated HUVECs were pretreated with vehicle (PBS, 60 min, control), 100 ng/ml toxin-B (60 min) or 50 μg/ml C3 transferase (16 h) washed and then incubated with human lymphocytes for 10 min at 37°C. Samples were fixed, stained, and analyzed as in A. Values represent mean ± SEM (n = 3–5).

We demonstrated previously that the endothelial projections both were enriched in, and required, F-actin (Carman et al., 2003). To assess the role of Rho family GTPases in projection formation, endothelial cells were pretreated with either *Clostridium diffucile* toxin-B, an inhibitor of Rho, Rac, and CDC42, or *Clostridium botulinum* C3 transferase, a selective inhibitor of Rho, under conditions that promoted similar deceases in actin stress fiber content, as assessed by phalloidin-FITC staining (unpublished data). For toxin-B this was associated with an approximately twofold reduction in both total projections and TEM (Fig. 8 B), whereas, C3 had no effect on either projections, as shown previously (Carman et al., 2003), or TEM in this setting (Fig. 8 B). As above (Fig. 8 A), in all cases the majority of TEM events (91%, 91%, and 93% for control,

toxin-B, and C3-treated samples, respectively) were projection positive (Fig. 8 B). These results imply a role for Rac and/or CDC42 in projection formation and provide correlative support for a functional role of projections in leukocyte diapedesis.

Discussion

We have performed high resolution imaging of the distribution dynamics of the critical adhesion receptors for diapedesis in an in vitro transmigration system. These studies reveal unambiguous usage of a transcellular route, in addition to the paracellular route, for diapedesis by considerable fractions of primary monocytes, neutrophils, and lymphocytes. Independent of the route, TEM events were demonstrated for the first time to be highly associated with endothelial cuplike structures enriched in ICAM-1 and VCAM-1 that surrounded the sites of diapedesis. These endothelial structures appeared to organize leukocyte β2- and α4-containing integrins into discrete linear clustering patterns oriented parallel to the direction of diapedesis that colocalized with the ICAM-1 and VCAM-1 projections. Finally, conditions that disrupted endothelial projections correlated with a two- to fourfold reduction in TEM. The results suggest that the projections may function to facilitate and guide TEM by forming a cuplike traction structure that is aligned parallel to the direction of transmigration.

The route taken by blood leukocytes as they cross the endothelium is of critical mechanistic and regulatory importance. Pioneering work by A. Dvorak and H. Dvorak (Feng et al., 1998, 2002) using serial-sectioning transmission EM provided unambiguous demonstration of the predominant use (at least in some settings) of the transcellular route of diapedesis in vivo. Similar observations have been made using serial-section transmission and/or scanning EM by others (Marchesi and Gowans, 1964; Faustmann and Dermietzel, 1985; Cho and De Bruyn, 1986; Fujita et al., 1991; Greenwood et al., 1994; Hoshi and Ushiki, 1999). Ironically, although in vivo scanning and serial-sectioning transmission EM have generally been accepted as proof for transcellular TEM, in vitro studies supporting paracellular TEM have apparently precluded general acceptance of this idea (Kvietys and Sandig, 2001; Muller, 2001). Our in vitro findings here with three distinct types of primary leukocytes coupled with previous studies using in vivo models (Marchesi and Gowans, 1964; Faustmann and Dermietzel, 1985; Cho and De Bruyn, 1986; Fujita et al., 1991; Greenwood et al., 1994; Feng et al., 1998, 2002; Hoshi and Ushiki, 1999) establish that a transcellular route for leukocyte diapedesis is likely to be an important and physiologically relevant phenomenon.

We suggest that our ability to detect transcellular TEM in this work is primarily a consequence of visualization of VE-cadherin (or PECAM-1) to discern junctions concomitantly with visualization of leukocyte integrins and their ligands on endothelium, to directly resolve the transendothelial passage. In addition, by using the highest resolution confocal imaging currently possible we were able to clearly visualize many transcellular TEM events that were in relatively close proximity to endothelial cell junctions (Fig. 7 A; Fig. S2 C). Even so, in some cases apparent transcellular TEM passages were too close to cell junctions for an unambiguous determination of the route and these events were scored as paracellular. Thus, our assessment of transcellular TEM may be underestimated.

A critical aspect of transcellular TEM that remains to be elucidated is the nature of the membrane fusion events underlying formation of the transcellular passageway. Caveolae and the vesiculo-vacuolar organelle are two well-documented dynamic and interrelated vesicular structures found in endothelial cells that are thought to function in transcellular permeability to fluid and solutes (Feng et al., 1996). These structures would seem ideal candidates for the membrane fusion elements required for pore formation in transcellular diapedesis (Feng et al., 2002). Our studies here show that caveolin-1 exhibits a modest, though unambiguous, enrichment at the periphery of the transcellular passage supporting a possible function for caveolae in transcellular diapedesis. Given this, it is noteworthy that the relatively low percentages of transcellular diapedesis observed here in vitro, compared with some in vivo studies (Feng et al., 2002), correlates with the relatively low levels of vesiculo-vacuolar organelle and caveolae in cultured endothelium compared with endothelium in vivo (Vasile et al., 1999).

We and others (Barreiro et al., 2002; Carman et al., 2003) have recently demonstrated that the endothelium proactively forms ICAM-1 and VCAM-1–enriched microvilli-like projections that form cuplike structures around populations of adherent leukocytes in an LFA-1– and VLA-4-dependent manner. These studies did not address whether projections were associated with diapedesis. However, in one of them it was interpreted that the endothelial projection structures likely functioned in adhesion strengthening and were incompatible with diapedesis and therefore would be required to disassemble before diapedesis could proceed (Barreiro et al., 2002).

To the contrary, based on both our previous (Carman et al., 2003) and current studies, we conclude that any functional role attributed to the endothelial projections would most likely lie in transmigration. The kinetics of projection formation are on the order of minutes (Carman et al., 2003), which is consistent with the time scale of diapedesis, but not with those of either rolling interactions (fractions of seconds) or firm adhesion (tens of seconds; Luu et al., 1999). Moreover, our analysis here demonstrates that transmigrating leukocytes represent the predominant projection-associated leukocyte population with an essentially complete correlation between TEM and the presence of projections. Finally, disruption of endothelial projections failed to alter the strength of the adhesions formed (Carman et al., 2003), but, as demonstrated here, correlated strongly with decreased efficiency of diapedesis. The finding that the subpopulations of projection-associated cells and transmigrating cells were essentially identical no matter whether monocytes, neutrophils, or lymphocytes were examined, or whether inhibitors were used, and that projections were highly associated with cells even at the very earliest detectable stages of TEM, suggests that projection formation is essential to the mechanism of diapedesis.

Based on this and the previously noted similarity to the phagocytic cup (Barreiro et al., 2002), we propose the nomenclature "transmigratory cup" to describe this novel cell–cell in-

terface architecture. Significantly, a variety of previous EM studies have made observations, including "endothelial microvilli" embracing transmigrating leukocytes, which is consistent with the formation of transmigratory cups in vivo (Williamson and Grisham, 1961; Faustmann and Dermietzel, 1985; Raine et al., 1990; Fujita et al., 1991).

We previously provided conclusive evidence that projection formation is the proactive response of the endothelium and does not require force or tension generation from the leukocyte (Carman et al., 2003). However, based on our analysis of asymmetrically distributed projections found associated with the trailing edge of laterally migrating leukocytes, we conclude that forces generated by leukocytes can modify the endothelial projections. Because asymmetric lateral projections were associated only with laterally migrating cells, and TEM was associated only with symmetric, cuplike endothelial projections, diapedesis would seems to require a transition from a highly polarized phenotype and rapid lateral migration to greater symmetry (in the x-y plane) and reduced lateral migration.

As discussed above, an important issue for TEM is how leukocytes establish directionality during diapedesis. The current model is that junctionally localized chemoattractant and adhesion molecule gradients provide the principle driving force for this (Bianchi et al., 1997; Aurrand-Lions et al., 2002; Muller, 2003). If we consider the transcellular migration events observed in this work, which occur at sites distant from endothelial junctions, we must conclude that an alternate "driving force" for TEM exists. The endothelial projections represent an attractive candidate for this. These vertical ICAM-1/VCAM-1–enriched microvilli-like projections form a cuplike traction structure that is aligned perpendicular to the plane of the endothelium and parallel to the direction of diapedesis, providing a physical basis for oriented migration. The finding that at sites opposing the endothelial projections, leukocyte integrins formed linear clusters reminiscent of fibrillar adhesions, on which cells are known exert forces during migration (Dzamba et al., 1994), is consistent with this idea. Given that chemoattractants are well known to be critical for TEM (Springer, 1994; Cinamon et al., 2001; Worthylake and Burridge, 2001) we envision that they cooperate with the ICAM-1– and VCAM-1–enriched transmigratory guidance structure in establishing proper directionality and, therefore, efficient TEM. In this regard, it is interesting to note that two prototypical chemokines, IL-8 and RANTES, have been shown to be distributed apically on endothelial microvilli in vivo (Middleton et al., 1997). Importantly, because the transmigratory cups were observed to be associated with virtually all TEM events, any functional consequences attributed to them should extend to both para- and transcellular TEM. In the case of paracellular TEM, projections would be anticipated to cooperate with other mechanisms previously shown to be functionally important (Bianchi et al., 1997; Aurrand-Lions et al., 2002; Muller, 2003).

Our studies demonstrate that leukocytes use transcellular, in addition to paracellular, routes for diapedesis. Independent of route, TEM events were highly associated with the transmigratory cup, in which ICAM-1– and VCAM-1–enriched vertical endothelial projections surround the site of leukocyte diapedesis. The architecture of this cup, and the high degree of correlation between these structures and the act of diapedesis, suggest that the transmigratory cup represents an important mode of directional guidance for TEM. The finding that both para- and transcellular TEM events by monocytes, neutrophils, and lymphocytes are associated with topologically similar transmigratory cups, demonstrates that this structure represents a general feature of TEM.

Materials and methods

Antibodies and reagents

Sources for antibodies to human αL (TS2/4), αM (CBRM1/23), β2 (CBR-LFA1/7), ICAM-1 (CBR-IC1/11), and ICAM-2 (CBR-IC2/1) have been described previously (Klickstein and Springer, 1995; Lu et al., 2001). Anti–CD14-FITC and control IgG2a-FITC were obtained from Immunotech. Anti–VE-cadherin (clone 55-7H1) and MCP-1 were obtained from BD Biosciences. Monoclonal anti-α4 (clone 7.2R) and anti–PECAM-1 (clone 9G11) and polyclonal anti–VCAM-1 and SDF-1 were obtained from R&D Systems. Fab fragments were prepared via papain cleavage according to the manufacturer's instructions (Pierce Chemical Co.). Antibody and Fab conjugation to Cy3, Cy5 (Amersham Biosciences), or Alexa 488 (Molecular Probes) bis-reactive dyes were according to manufacturer's instructions. PAF was obtained from Calbiochem. BAPTA-AM, colchicine, cytochalasin-D, and heparin were obtained from Sigma-Aldrich. Clostridium diffucile toxin-B was obtained from List Biochemicals. Clostridium botulinum C3 transferase was a gift provided by J. Greenwood and P. Adamson (University College of London, London, UK).

Cells and cell culture

HUVECs, neutrophils, peripheral blood mononuclear cells, and monocytes were purified and cultured as described previously (Carman et al., 2003). Lymphocytes were prepared by adsorbing the monocytes to gelatin-coated plates and culturing nonadherent lymphocytes in RPMI supplemented with 10% FBS and PHA (1 μg/ml) for 3 d, followed by culture in IL-2 (20 ng/ml) for 3–6 d. Flow cytometic analysis demonstrated that these cells were 97% CD3 positive. HUVEC transient transfection was performed by Amaxa nucleofection according to the manufacturer's instructions (Amaxa Inc.). DNA expression constructs for Caveolin-1-GFP and GFP-caveolin-1 were provided by M. Lisanti (Albert Einstein College of Medicine, Bronx, NY).

Adhesion and TEM experiments

For most fluorescence microscopy experiments, HUVECs were plated at 90% confluency on fibronectin (10 μg/ml)-coated polystyrene or glass surfaces and cultured for 48–72 h before use. HUVECs grown on gelatin or Matrigel gave results indistinguishable from those on fibronectin. Before each experiment, HUVECs were activated for 12 h with TNF-α (100 ng/ml). Immediately before addition of leukocytes, HUVECs were incubated with either PAF (100 nm), MCP-1 (200 ng/ml), or SDF-1 (200 ng/ml) at 37°C for 20 min. Where indicated, HUVECs were also preincubated with BAPTA-AM (20 μM, 1 h), colchicine (10 μM, 20 min), toxin-B (100 ng/ml, 1 h), C3 transferase (50 μg/ml, 16 h), or appropriate dilutions of vehicle (DMSO or PBS) concomitant with chemoattractant. In all cases, HUVECs were washed five times before addition of leukocytes with HBSS supplemented with 20 mM Hepes, pH 7.2, and 1% human serum albumin (buffer A). Freshly isolated neutrophils or monocytes or IL-2 cultured lymphocytes were washed and resuspended in buffer A and then added to HUVEC monolayers and incubated at 37°C for the indicated times. Cells were imaged live in Bioptechs chambers maintained at 37°C, or fixed in 3.7% formaldehyde in PBS for 5 min, stained for β2 (LFA1/7-Cy3 or -Cy5; 20 μg/ml), αL (TS2/4-Cy3; 20 μg/ml), αM (CBRM1/23-Cy3; 20 μg/ml), α4 (R7.2-488; 20 μg/ml), ICAM-1 (IC1/11-488, IC1/11-Fab-488, or IC1/11-Cy3; 20 μg/ml), ICAM-2 (IC2/1-488 or Cy3; 20 μg/ml), VCAM-1 (polyclonal anti–VCAM-1-Cy3; 20 μg/ml), PECAM-1 (9G11-Cy3), VE-cadherin (55-7H1-Cy3 or -Cy5; 20 μg/ml) in PBS for 20 min at RT and then washed three times with PBS before imaging. For live-cell experiments, endothelial cells were preincubated with nonfunction blocking IC1/11-Fab-488 (20 μg/ml) for 20 min and then washed before addition of leukocytes that were prelabeled with 5-(and-6)-chloromethyl SNARF-1, acetate (Molecular Probes) according to the manufacturer's instructions.

For shear experiments, HUVEC monolayers were assembled as the lower wall in a parallel-wall flow chamber in a 37°C warm room. Leukocytes, in buffer A, were infused at 0.3 dyne/cm^2 for 30 s, to allow accumulation, then subjected to 4 dyne/cm^2 shear force for 10 min and finally fixed by perfusion of buffer A/3.7% formaldehyde under the same shear. Cells were stained as above.

Image acquisition and processing

Wide field differential interference contrast, IRM, and fluorescence imaging was conducted on an Axiovert S200 epifluorescence microscope (Carl Zeiss MicroImaging, Inc.), using a 63× oil objective, coupled to a Hamamatsu Orca CCD. Confocal imaging was performed with a Radiance 2000 Laser-scanning confocal system (Bio-Rad Laboratories) on a microscope (model BX50BWI; Olympus) with a 100× water immersion objective. For serial Z-stacks the section thickness was between 0.1 and 0.3 μm. Image processing, including background subtraction and digital deconvolution, was performed with Openlab software (Improvision). Three dimensional reconstruction and projection of Z-stacks was performed with VoxBlast software (Vay Tek). Images were then exported to Photoshop or Quicktime software for preparation of final images or videos, respectively.

Criteria for determination of leukocyte TEM

Criteria for determination of leukocyte TEM were based on analysis of the relative distribution of ICAM-1, LFA-1, and VE-cadherin fluorescence in both the x-y and the z dimensions. The point of leukocyte penetration through the endothelium (the TEM passage) was defined by the region in the x-y dimension completely devoid of ICAM-1 fluorescence in all z-planes. The TEM passage contained leukocyte LFA-1 fluorescence that extended down to the most basal sections at the substrate. LFA-1 fluorescence adjacent to the TEM passage that was below that of ICAM-1 was taken to indicate portions of the leukocytes that had spread underneath the endothelium. The validity of our ICAM-1/LFA-1–based analysis of TEM was confirmed by parallel experiments that compared the localization of HUVEC stress fibers with leukocyte LFA-1 as described previously (Sandig et al., 1997). Further validation for our method came from IRM, which confirmed that portions of leukocytes determined by ICAM-1/LFA-1 fluorescence to have penetrated the endothelium were in close contact with the substrate, whereas the apical portions of the leukocytes were confirmed not to be in contact with the substrate. TEM adjacent to VE-cadherin-stained endothelial cell–cell junctions was scored as paracellular; TEM where no part of the TEM passage was within 1 μm of a junction was scored as transcellular.

Cells were scored as either adherent but not transmigrating, in TEM stage-1, -2, or -3 or under the endothelium. In addition, each cell was scored for the presence of significant ICAM-1–enriched vertical projections of 1 μm in length or greater. Projections associated with only one side of a leukocyte were termed "asymmetric" or "tetherlike", whereas those that were associated with at least 240° of the circumference of a leukocyte were termed "symmetric" or "cuplike".

Online supplemental material

Figs. S1–S3 show further examples of both para- and transcellular transmigratory cups with monocytes, neutrophils, and lymphocytes under static (1–2) and shear (3) conditions. Fig. S4 depicts distribution of ICAM-2, PECAM-1, and VE-cadherin relative to transmigratory cups. Fig. S5 shows ICAM-1 projections associated with sub-endothelial leukocytes. Video 1 shows three-dimensional rotation of the images depicted in Fig. 6 C. Online supplemental materials are available at http://www.jcb.org/cgi/content/full/jcb.200404129/DC1.

This work was supported by a fellowship (C.V. Carman) and a grant (T.A. Springer) from the National Institutes of Health.

Submitted: 26 April 2004
Accepted: 9 September 2004

References

Adamson, P., S. Etienne, P.O. Couraud, V. Calder, and J. Greenwood. 1999. Lymphocyte migration through brain endothelial cell monolayers involves signaling through endothelial ICAM-1 via a rho-dependent pathway. *J. Immunol.* 162:2964–2973.

Aurrand-Lions, M., C. Johnson-Leger, and B.A. Imhof. 2002. The last molecular fortress in leukocyte trans-endothelial migration. *Nat. Immunol.* 3:116–118.

Baekkevold, E.S., T. Yamanaka, R.T. Palframan, H.S. Carlsen, F.P. Reinholt, U.H. von Andrian, P. Brandtzaeg, and G. Haraldsen. 2001. The CCR7 ligand elc (CCL19) is transcytosed in high endothelial venules and mediates T cell recruitment. *J. Exp. Med.* 193:1105–1112.

Barreiro, O., M. Yanez-Mo, J.M. Serrador, M.C. Montoya, M. Vicente-Manzanares, R. Tejedor, H. Furthmayr, and F. Sanchez-Madrid. 2002. Dynamic interaction of VCAM-1 and ICAM-1 with moesin and ezrin in a novel endothelial docking structure for adherent leukocytes. *J. Cell Biol.* 157:1233–1245.

Bianchi, E., J.R. Bender, F. Blasi, and R. Pardi. 1997. Through and beyond the wall: late steps in leukocyte transendothelial migration. *Immunol. Today.* 18:586–591.

Carman, C.V., C.-D. Jun, A. Salas, and T.A. Springer. 2003. Endothelial cells proactively form microvilli-like membrane projections upon ICAM-1 engagement of leukocyte LFA-11. *J. Immunol.* 171:6135–6144.

Chen, S., and T.A. Springer. 1999. An automatic braking system that stabilizes leukocyte rolling by an increase in selectin bond number with shear. *J. Cell Biol.* 144:185–200.

Cho, Y., and P.P. De Bruyn. 1986. Internal structure of the postcapillary high-endothelial venules of rodent lymph nodes and Peyer's patches and the transendothelial lymphocyte passage. *Am. J. Anat.* 177:481–490.

Cinamon, G., V. Shinder, and R. Alon. 2001. Shear forces promote lymphocyte migration across vascular endothelium bearing apical chemokines. *Nat. Immunol.* 2:515–522.

Dzamba, B.J., H. Bultmann, S.K. Akiyama, and D.M. Peters. 1994. Substrate-specific binding of the amino terminus of fibronectin to an integrin complex in focal adhesions. *J. Biol. Chem.* 269:19646–19652.

Etienne-Manneville, S., J.B. Manneville, P. Adamson, B. Wilbourn, J. Greenwood, and P.O. Couraud. 2000. ICAM-1-coupled cytoskeletal rearrangements and transendothelial lymphocyte migration involve intracellular calcium signaling in brain endothelial cell lines. *J. Immunol.* 165:3375–3383.

Faustmann, P.M., and R. Dermietzel. 1985. Extravasation of polymorphonuclear leukocytes from the cerebral microvasculature. Inflammatory response induced by alpha-bungarotoxin. *Cell Tissue Res.* 242:399–407.

Feng, D., J.A. Nagy, J. Hipp, H.F. Dvorak, and A.M. Dvorak. 1996. Vesiculovacuolar organelles and the regulation of venule permeability to macromolecules by vascular permeability factor, histamine, and serotonin. *J. Exp. Med.* 183:1981–1986.

Feng, D., J.A. Nagy, K. Pyne, H.F. Dvorak, and A.M. Dvorak. 1998. Neutrophils emigrate from venules by a transendothelial cell pathway in response to FMLP. *J. Exp. Med.* 187:903–915.

Feng, D., J.A. Nagy, H.F. Dvorak, and A.M. Dvorak. 2002. Ultrastructural studies define soluble macromolecular, particulate, and cellular transendothelial cell pathways in venules, lymphatic vessels, and tumor-associated microvessels in man and animals. *Microsc. Res. Tech.* 57:289–326.

Fujita, S., R.K. Puri, Z.X. Yu, W.D. Travis, and V.J. Ferrans. 1991. An ultrastructural study of in vivo interactions between lymphocytes and endothelial cells in the pathogenesis of the vascular leak syndrome induced by interleukin-2. *Cancer.* 68:2169–2174.

Greenwood, J., R. Howes, and S. Lightman. 1994. The blood-retinal barrier in experimental autoimmune uveoretinitis. Leukocyte interactions and functional damage. *Lab. Invest.* 70:39–52.

Greenwood, J., Y. Wang, and V.L. Calder. 1995. Lymphocyte adhesion and transendothelial migration in the central nervous system: the role of LFA-1, ICAM-1, VLA-4 and VCAM-1. *Immunology.* 86:408–415.

Hoshi, O., and T. Ushiki. 1999. Scanning electron microscopic studies on the route of neutrophil extravasation in the mouse after exposure to the chemotactic peptide N-formyl-methionyl-leucyl-phenylalanine (fMLP). *Arch. Histol. Cytol.* 62:253–260.

Huang, A.J., J.E. Manning, T.M. Bandak, M.C. Ratau, K.R. Hanser, and S.C. Silverstein. 1993. Endothelial cell cytosolic free calcium regulates neutrophil migration across monolayers of endothelial cells. *J. Cell Biol.* 120:1371–1380.

Klickstein, L.B., and T.A. Springer. 1995. CD54 (ICAM-1) cluster report. *In* Leucocyte Typing V: White Cell Differentiation Antigens. S. F. Schlossman, L. Boumsell, W. Gilks, J. Harlan, T. Kishimoto, T. Morimoto, J. Ritz, S. Shaw, R. Silverstein, T. Springer, et al., editors. Oxford University Press, New York. 1548–1550.

Kvietys, P.R., and M. Sandig. 2001. Neutrophil diapedesis: paracellular or transcellular? *News Physiol. Sci.* 16:15–19.

Lampugnani, M.G., M. Resnati, M. Raiteri, R. Pigott, A. Pisacane, G. Houen, L.P. Ruco, and E. Dejana. 1992. A novel endothelial-specific membrane protein is a marker of cell–cell contacts. *J. Cell Biol.* 118:1511–1522.

Lu, C., M. Shimaoka, Q. Zang, J. Takagi, and T.A. Springer. 2001. Locking in alternate conformations of the integrin αLβ2 I domain with disulfide bonds reveals functional relationships among integrin domains. *Proc. Natl. Acad. Sci. USA.* 98:2393–2398.

Luscinskas, F.W., G.S. Kansas, H. Ding, P. Pizcueta, B.E. Schleiffenbaum, T.F. Tedder, and M.A. Gimbrone Jr. 1994. Monocyte rolling, arrest and spreading on IL-4–activated vascular endothelium under flow is mediated via sequential action of L-selectin, β_1-integrins, and β_2-integrins. *J. Cell Biol.* 125:1417–1427.

Luu, N.T., G.E. Rainger, and G.B. Nash. 1999. Kinetics of the different steps during neutrophil migration through cultured endothelial monolayers treated with tumour necrosis factor-alpha. *J. Vasc. Res.* 36:477–485.

Marchesi, V.T., and J.L. Gowans. 1964. The migration of lymphocytes through the endothelium of venules in lymph nodes: an electron microscope study. *Proc. R. Soc. Lond. B. Biol. Sci.* 159:283–290.

Middleton, J., S. Neil, J. Wintle, I. Clark-Lewis, H. Moore, C. Lam, M. Auer, E. Hub, and A. Rot. 1997. Transcytosis and surface presentation of IL-8 by venular endothelial cells. *Cell.* 91:385–395.

Muller, W.A. 2001. Migration of leukocytes across endothelial junctions: some concepts and controversies. *Microcirculation.* 8:181–193.

Muller, W.A. 2003. Leukocyte-endothelial-cell interactions in leukocyte transmigration and the inflammatory response. *Trends Immunol.* 24:327–334.

Oppenheimer-Marks, N., L.S. Davis, D.T. Bogue, J. Ramberg, and P.E. Lipsky. 1991. Differential utilization of ICAM-1 and VCAM-1 during the adhesion and transendothelial migration of human T lymphocytes. *J. Immunol.* 147:2913–2921.

Raine, C.S., B. Cannella, A.M. Duijvestijn, and A.H. Cross. 1990. Homing to central nervous system vasculature by antigen-specific lymphocytes. II. Lymphocyte/endothelial cell adhesion during the initial stages of autoimmune demyelination. *Lab. Invest.* 63:476–489.

Ross, R. 1999. Atherosclerosis-an inflammatory disease. *N. Engl. J. Med.* 340: 115–126.

Sandig, M., E. Negrou, and K.A. Rogers. 1997. Changes in the distribution of LFA-1, catenins, and F-actin during transendothelial migration of monocytes in culture. *J. Cell Sci.* 110:2807–2818.

Springer, T.A. 1994. Traffic signals for lymphocyte recirculation and leukocyte emigration: the multi-step paradigm. *Cell.* 76:301–314.

Strey, A., A. Janning, H. Barth, and V. Gerke. 2002. Endothelial Rho signaling is required for monocyte transendothelial migration. *FEBS Lett.* 517: 261–266.

Vasile, E., H. Qu, H.F. Dvorak, and A.M. Dvorak. 1999. Caveolae and vesiculovacuolar organelles in bovine capillary endothelial cells cultured with VPF/VEGF on floating Matrigel-collagen gels. *J. Histochem. Cytochem.* 47:159–167.

Williamson, J.R., and J.W. Grisham. 1961. Electron microscopy of leukocytic margination and emigration in acute inflammation in dog pancreas. *Am. J. Pathol.* 39:239–256.

Worthylake, R.A., and K. Burridge. 2001. Leukocyte transendothelial migration: orchestrating the underlying molecular machinery. *Curr. Opin. Cell Biol.* 13:569–577.

were pretreated with vehicle (DMSO, 60 min), 10 μm colchicine (20 min) or 20 μm BAPTA-AM (60 min) washed and then incubated with monocytes for 10 minutes at 37ºC. Cells were fixed, stained for ICAM-1 (IC1/11-488; green) and LFA-1 (CBR-LFA1/7-Cy3; red) and then analyzed by confocal microscopy. In each of three to five separate experiments at least 100 monocytes in randomly selected fields were carefully analyzed in all apical to basal planes and scored for the presence of significant ICAM-1-enriched projections of 1 μm in length or greater and as being either apically adherent ('A'), in the process of TEM (including both para- and trans-cellular events and TEM 1-3) ('T') or under ('U') the HUVEC monolayer. Each bar represents the percentage of total cells scored for each experimental condition (DMSO, colchicine or BAPTA-AM) in each of the three categories. The black portion of each bar is the fraction of cells positive for associated ICAM-1 projections. The gray portion of each bar is the fraction of the cells that were negative for the presence of ICAM-1 projections. B. TNF-α-activated, SDF-1-pretreated HUVECs were pretreated with vehicle (PBS, 60 min;'control'), 100 ng/ml toxin-B (60 min) or 50 μg/ml C3 transferase (16 hours) washed and then incubated with human lymphocytes for 10 minutes at 37ºC. Samples were fixed, stained and analyzed as in A. Values represent mean ± SEM (n=3-5).

Online Supplementary Material Figure Legends

Supplemental Figure 1. Monocytes transmigrate via both para- and trans-cellular routes in association with ICAM-1 projections. TNF-α-activated HUVECs were pre-treated with MCP-1 and then incubated with freshly isolated monocytes for 20 minutes. Cells were then fixed and stained for (IC1/11-Fab-488; green), LFA-1 (CBR-LFA1/7-Cy3; red) and VE-cadherin (55-7H1-Cy5; blue) (shown in A only) and imaged by confocal microscopy. A representative image depicts two monocytes migrating via either a para-

cellular (1) (TEM stage 2) or a trans-cellular route (2) (TEM stage 1). B. Side views of cross-sections of cells 1 and 2. C. Higher magnification of boxed regions in A (cells 1 and 2) projected using only the apical sections (brackets in B). Scale bar represents 5 μm.

Supplemental Figure 2. Neutrophils, lymphocytes and monocytes migrate across the endothelium via both trans- and para-cellular routes in association with ICAM-1 projections. TNF-α-activated HUVECs were pre-treated with PAF, SDF-1 or MCP-1 and then incubated with freshly isolated neutrophils, cultured primary lymphocytes or monocytes, respectively, for 10-20 minutes. Cells were then fixed and stained for ICAM-1 (CBRIC1/11-488; green), LFA-1 (CBR-LFA1/7-Cy3; red) and VE-cadherin (55-7H1-Cy5; blue) (shown in upper panels only) and imaged by confocal microscopy. A and B. Upper panels represent top view projections of transmigrating leukocytes. Lower panels represent side view projections of cross-sections boxed in upper panels. A. Representative neutrophils migrating via para-(left) and trans-(right) cellular routes in stage TEM-2 and TEM-1, respectively. B. Representative lymphocytes migrating via para-(left) and trans-(right) cellular routes in stage TEM-2. C. Monocyte transmigrating through a trans-cellular route in relatively close proximity to the endothelial junction. Left panel represents top view projection of the apical confocal sections. Middle and right panels represent top view projections of all confocal sections. The edge of one endothelial cell (black), the VE-cadherin-stained adherence junction (blue), the perimeter of the monocyte and ICAM-1 projections (white), and the trans-cellular migration passage (red) have been highlighted in the right panel. The black double-headed arrow represents the space separating the TEM passage and the adherence junction and is approximately one micron. This image represents the limit of resolution of trans-cellular

TEM. Events in which the TEM passage was only slightly closer to the adherence junctions were scored as para-cellular. Scale bar represents 5 μm.

Supplementary Figure 3. ICAM-1-enriched endothelial cup-like structures are associated with transmigrating lymphocytes, monocytes and neutrophils under shear. Primary cultured lymphocytes (A) or freshly isolated monocytes (B) or neutrophils (C) were allowed to transmigrate across TNF-α-activated HUVEC monolayers for 10 minutes under 4 dynes/cm^2 shear stress and then fixed and stained according to *Materials and Methods*. ICAM-1 (IC1, green), LFA-1 (β2, red) and VE-cadherin (VE-CAD, blue) are shown for representative para-(A) and trans-(B and C) cellular migration events as both top view (upper panels) and side view (lower panels) projections. Scale bar represents 5 μm.

Supplemental Figure 4. ICAM-2 and PECAM-1 are weakly associated and VE-cadherin is not associated with projections surrounding sites of transmigration. A. Top view of confocal sections of a monocyte in TEM-1 at 0 μm (upper panels) and 3 μm (lower panels) above the apical endothelial surface. ICAM-1 (IC1; green), ICAM-2 (IC2; red), and β2 integrin (β2; blue) are shown either separately (left and middle panels) or merged (right). B. Top view confocal sections of a monocyte in TEM-1 at 0 μm (upper panels) and 3 μm (lower panels) above the apical endothelial surface. ICAM-1 (IC1; green), PECAM-1 (red), and β2 integrin (β2; blue) are shown either separately (left and middle panels) or merged (right). Scale bar represents 5 μm. Note that the fluorescence of PECAM-1 is brighter than ICAM-1 in the 0 μm section and markedly lower than ICAM-1 in the 3 μm section in which projections are present. C. Top view of confocal sections of a monocyte in TEM-1 at 0 μm (upper panels) and 3 μm (lower panels) above the

apical endothelial surface. ICAM-1 (IC1; green), VE-cadherin (VE-CAD; red), and β2 integrin (β2; blue) are shown either separately (left and middle panels) or merged (right). Note that VE-cadherin staining at 0 μm is discontinuous at the TEM passage in contrast Fig. 6B, and that VE-cadherin staining is absent in the 3 μm section.

Supplemental Figure 5. At final stages of TEM, ICAM-1 projections are pulled to the basal side of the endothelium by the uropod of the advancing leukocyte. TNF-α-activated HUVECs were pre-treated with MCP-1 and then incubated with freshly isolated monocytes for 20 minutes. Cells were then fixed and stained for ICAM-1, (IC1/11-488; green), LFA-1 (CBR-LFA1/7-Cy3; red) and imaged by confocal microscopy. A, D, G. Three representative monocytes at slightly different late stages of para-cellular (A and D) or trans-cellular (G) TEM are shown. Images represent top views of selected basal sections of β2 integrin (upper panels), ICAM-1 (green; middle panels) or both merged (lower panels). B, E, H. Side views of boxed cross sections indicated in A, D and G, respectively. C, F, I. Dotted, dashed and solid line represent the edges of the sub-endothelial leukocyte membrane, the perimeter of the ICAM-1 projections and the TEM passage, respectively, of the cells shown in A, D and G. Scale bar represents 5 μm.

Supplemental Video 1. Three-dimensional rotation of the ICAM-1- and VCAM-1 enriched endothelial "transmigratory-cup". In order to enhance the visualization of the architecture of the ICAM-1- and VCAM-1-enriched endothelial membrane projections and the co-localized linear tracks of leukocyte LFA-1, the serial confocal sections of monocyte TEM depicted in Figure 6C were rendered as a series of 30 three-dimensional projections, each representing successive rotation about both the X- and Z-axis in 3° intervals for a total of 90° about each axis. These projections are depicted sequentially as

a Quicktime video. VCAM-1 (upper left panel; red), ICAM-1 (upper right panel; green) and β2 integrin (lower left panel; blue) are shown either separately (upper panels and lower left panel) or merged (lower right panel).

Carman_Supplemental1

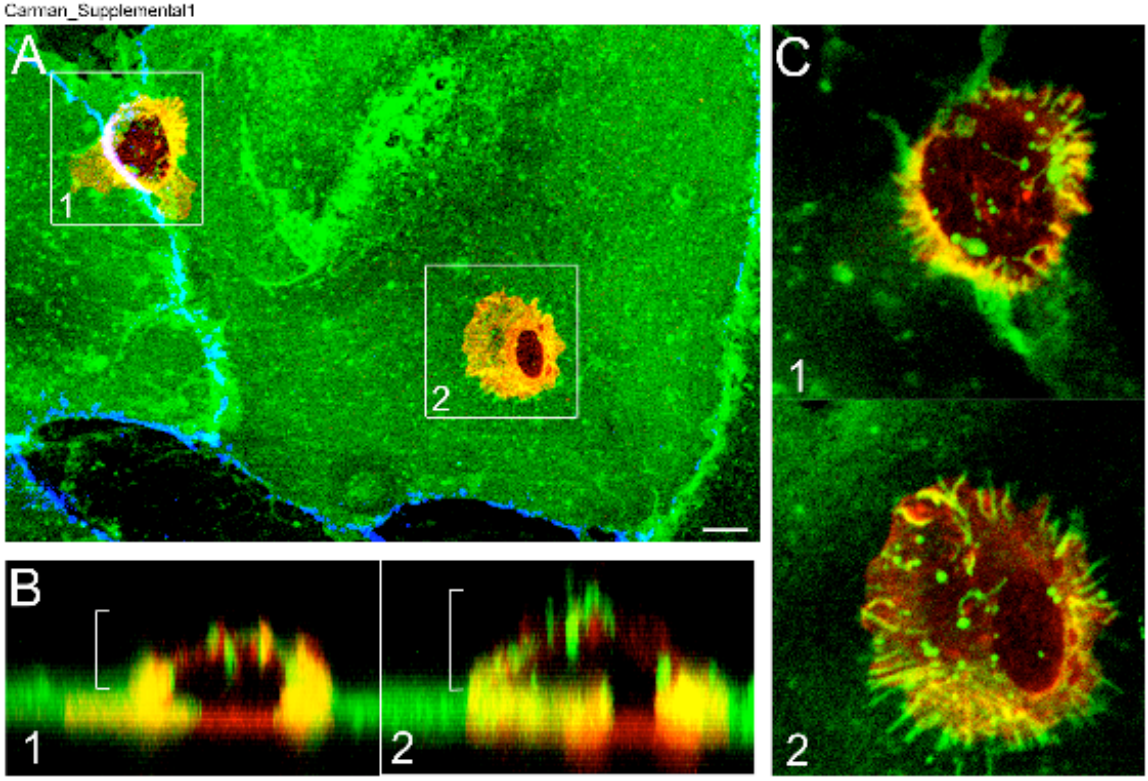

Carman_Supplemental2

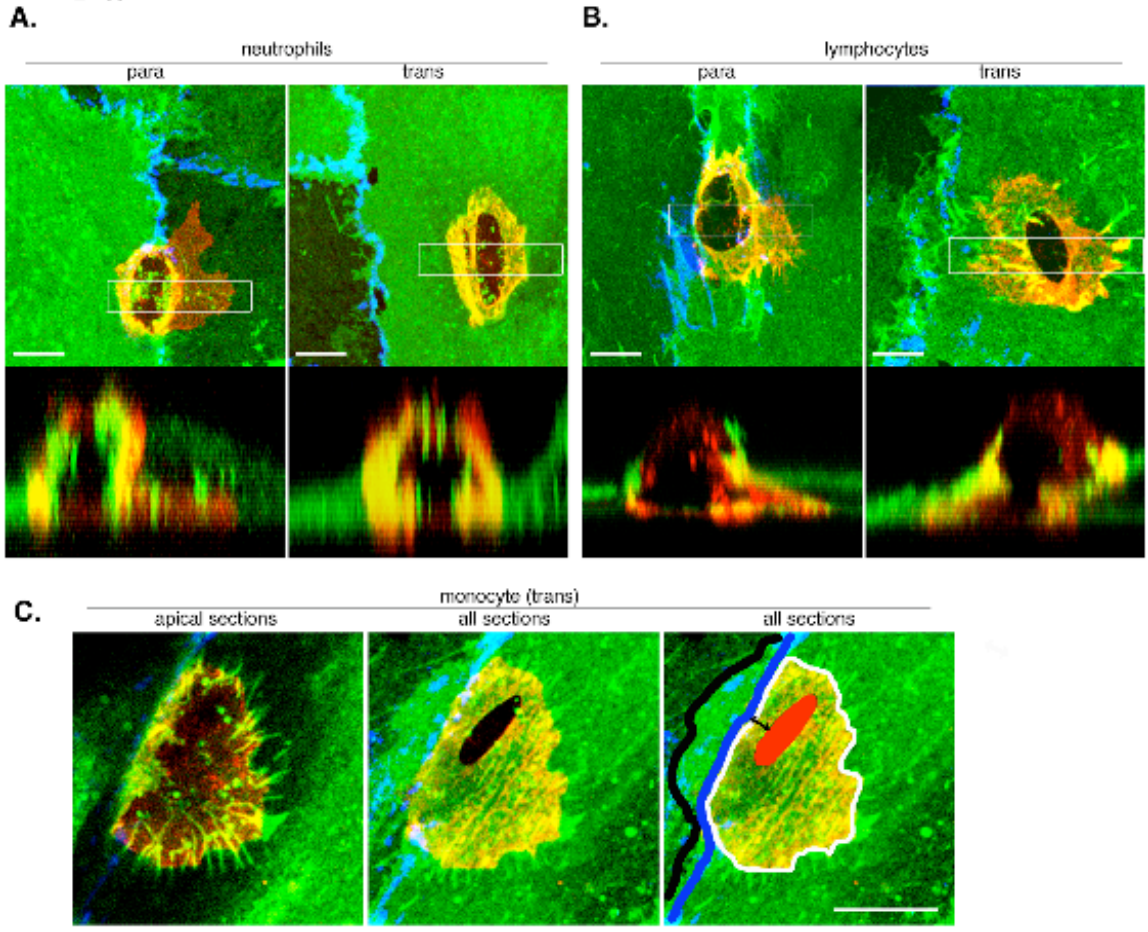

Carman_Supplemental3

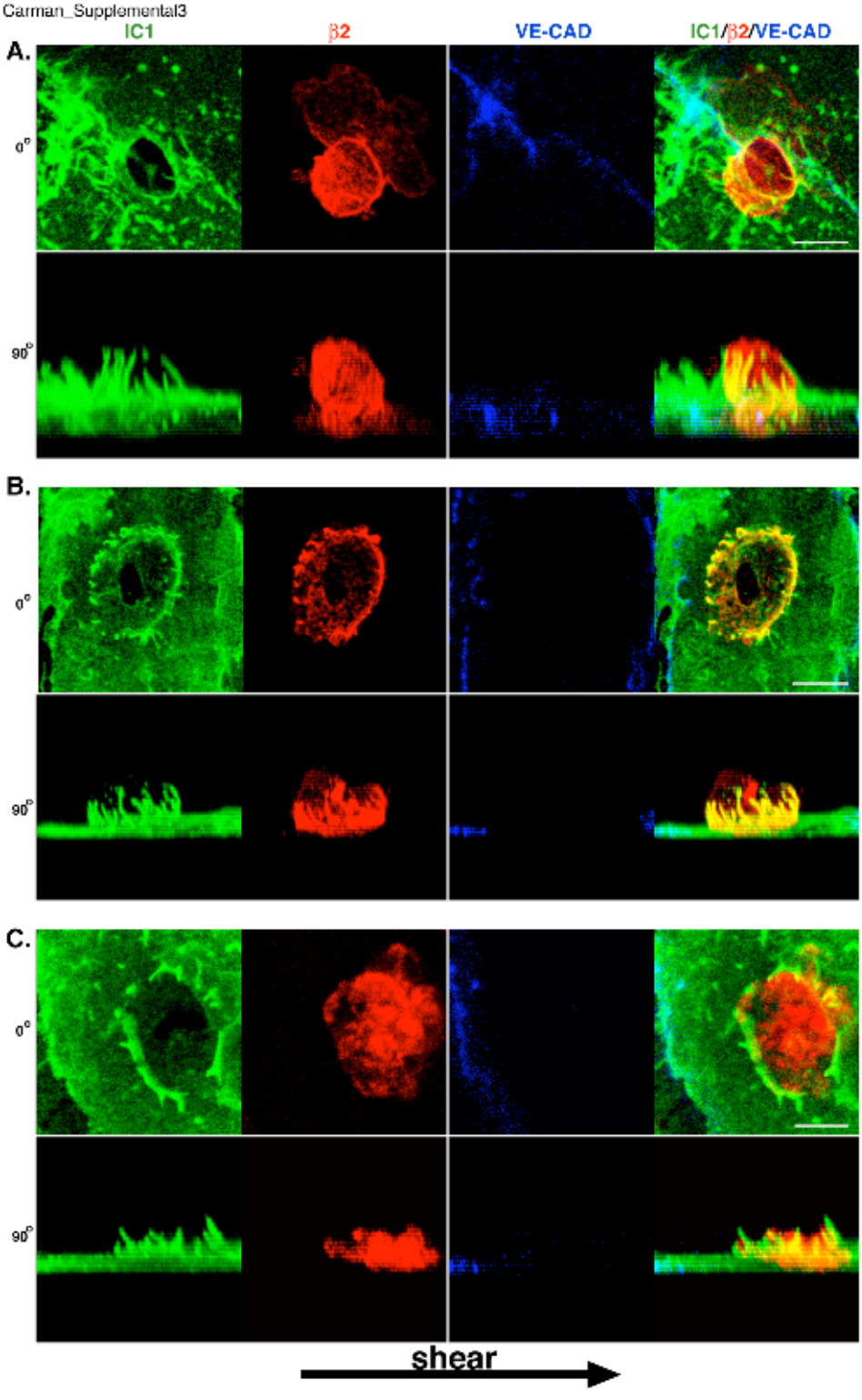

Carman_Supplemental4

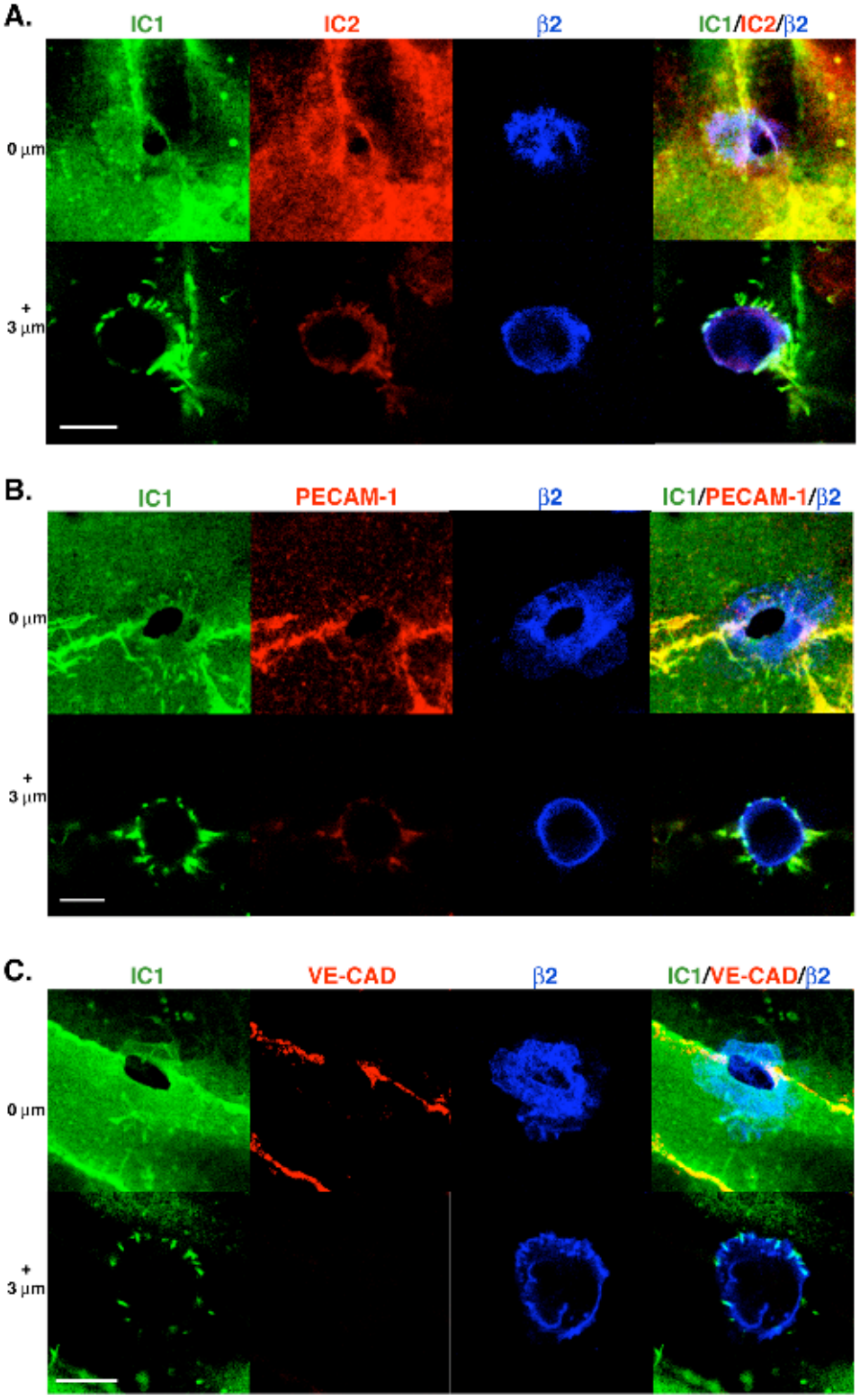

Carman_Supplemental5